Dynamics of Single-Atom Motion Observed in a High-Finesse Cavity

P. Münstermann, T. Fischer, P. Maunz, P. W. H. Pinkse, and G. Rempe
Fakultät für Physik, Universität Konstanz, D-78457 Konstanz, Germany
(Received 30 November 1998)

We investigate mechanical forces on single atoms in a high-finesse optical cavity containing less than one photon on average. We count the number of atoms strongly coupled to the cavity mode close to an antinode and measure the intensity autocorrelation function of the pump light transmitted through the cavity. Distinct features are observed and attributed to the dipole force, diffusion, and velocity-dependent force, as predicted by the work of Horak *et al.* Our data agree well with the results of a Monte Carlo simulation. [S0031-9007(99)09150-4]

PACS numbers: 42.50.Ct, 32.80.Pj, 42.50.Vk

High-finesse cavities are well suited to examine quantum-electrodynamic (QED) effects in the interaction of a single atom and a single photon. Indeed, dramatic effects on the radiative properties of the atom have been observed [1]. However, the atomic momentum was usually assumed fixed: dynamics was considered to be electrodynamics. Mechanical forces in cavity QED, arising from the dipole potential, became important only after laser-cooling techniques allowed one to prepare atoms at ultralow temperatures. New phenomena were predicted, such as diffraction [2], reflection [3], trapping [4], and photon emission of a wave [5] of excited atoms by means of the cavity vacuum field.

As reported recently [6], these effects can now be investigated in the optical domain, where light forces are stronger than in the microwave domain originally considered. However, spontaneous decay and cavity losses are larger, too, so that the excitation must be continuously replenished by an external laser. The presence of dissipation leads to new, nonconservative forces [7]. As a prime example, a force proportional to the atomic velocity was predicted [8] for a strongly coupled atom-cavity system, where a single photon can repetitively be emitted and reabsorbed by the atom. The new force can be visualized in terms of a cavity-mediated Sisyphus mechanism, taking into account only the (dressed or Jaynes-Cummings) ground state and the first two states in which a single quantum of excitation is shared by the atom and the cavity: starting, e.g., in the ground state, the system is transferred to one of the two excited states by absorbing a photon from the external laser. The energy of the excited state depends on the atom-field coupling strength, which in turn depends on the atom's position in a standing-wave cavity. Because of the nonzero atomic velocity, the system adiabatically follows the excited state, thereby gaining or losing kinetic energy before it decays back to the ground state, whose energy does not depend on the position of the atom. Repetitive excitation and decay therefore leads to heating or cooling. Of course, the random jumps between the states leads to diffusion, which heats the atom.

We point out that the forces considered in this Letter work in a system where the energy levels are fixed by the atom and cavity parameters, while the externally applied laser field determines the population of these levels. Interestingly, cooling and heating are predicted also for red and blue detuning, respectively, in contrast to the ordinary Sisyphus mechanism in an intense classical field [9,10]. In addition, the potentially long cavity decay time might allow one to reach sub-Doppler temperatures even for a two-level atom. The new velocity-dependent force has not been observed up till now.

In this Letter we study cavity-QED forces on single atoms passing one after the other through a weakly driven high-finesse optical resonator. From measurements of the number of atoms detected close to an antinode of the standing-wave cavity field, we find that a significant fraction of atoms is repelled from a blue-detuned cavity mode. Moreover, the intensity autocorrelation function of the transmitted light reveals rich dynamics of the atomic motion. Quantitatively, the data of both measurements are well understood with a Monte Carlo simulation based on the forces predicted in Refs. [8].

Our experiments are performed in the strong-coupling regime, where the oscillatory exchange of a single quantum of excitation between the cavity and the atom, characterized by twice the optimum coupling g_0, is faster than the decay rates of the atomic dipole γ and the cavity field κ. Our parameters are $(g_0, \gamma, \kappa) = 2\pi \times (16, 3, 1.5)$ MHz. Interaction times exceeding 100 μs are achieved with an atomic fountain as a cold atom source.

The experimental setup has been described in Ref. [11] and is shown in the left part of Fig. 1. ^{85}Rb atoms are collected in a magneto-optical trap (MOT) and further cooled in optical molasses to ≈ 5 μK. Introducing a frequency shift between the upper and the lower trapping beams creates a moving molasses that launches the atoms in a fountain burst towards the cavity 25 cm straight above the MOT. For each burst, new atoms are collected. By varying the trapping and launching parameters, the number and the vertical velocity of the atoms can be tuned. Before entering the cavity (finesse 4.3×10^5, length 116 μm, mode function $\psi(\vec{r}) = \cos(2\pi z/\lambda) \exp[-(x^2 + y^2)/w_0^2]$, with $w_0 = 29$ μm), the atoms are optically pumped into the $F = 3, m_F = 3$ ground state. The cavity

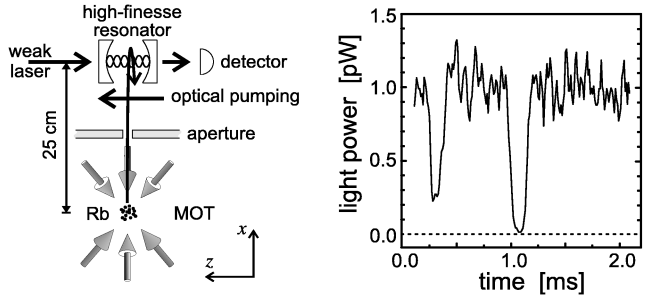

FIG. 1. Left: Experimental setup. Right: Transmitted power. Two minima (dips) are clearly visible, each indicating the passage of a single atom. A transmitted power of 1 pW corresponds, on average, to 1.1 intracavity photons.

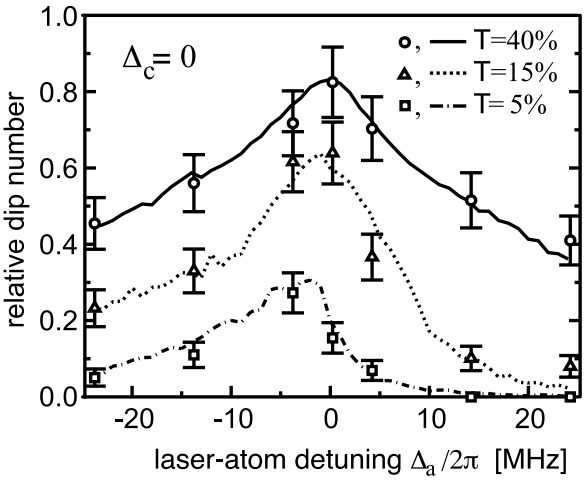

FIG. 2. Experimental (symbols) and numerical results (curves) on the relative number of dips dropping below a fraction $\mathcal{T}$ of the empty-cavity transmission versus Δ_a. Without atoms, the cavity contains 1.1 photons on average.

mode is excited with circularly polarized light from a weak laser beam near resonant with the $5^2S_{1/2}$, $F = 3 \leftrightarrow 5^2P_{3/2}$, $F = 4$ transition of the atoms at $\lambda = 780$ nm. The frequencies of the laser and the resonances of the cavity and the atom are ω_l, ω_c, and ω_a, respectively, known within $\pm 2\pi \times 0.5$ MHz. The photons transmitted through the cavity are recorded with a sensitive single-photon counter. Without atoms, the mean intracavity photon number is always less than 1.1.

With the laser and the cavity both on resonance with the atoms, single atoms passing through the cavity reduce the transmitted power. A typical real-time recording of this effect is shown in the right part of Fig. 1. The displayed signal is obtained by integrating the photon counts over 10 μs and averaging each data point with its left and its right neighbors. The signal has two pronounced minima (dips) at times $\approx$0.3 ms and $\approx$1.1 ms. Each dip is caused by an atom passing the cavity mode with a velocity of 0.55 m/s. The minimum transmission in a dip depends on $g(\vec{r}) = g_0\psi(\vec{r})$ and the actual trajectory $\vec{r}(t)$ taken. Atoms moving through an antinode of the cavity cause deeper dips than atoms passing the cavity somewhere else [6,11–13].

Before entering the cavity, the kinetic energy of the atoms along the cavity axis is 3 orders of magnitude smaller than $\hbar g_0$. Therefore, the atomic trajectories can significantly be modified by the dipole force, even for light fields with less than one photon on average. To investigate this, the light field is detuned from the atomic resonance, $\Delta_a \equiv \omega_l - \omega_a \neq 0$. The cavity is prepared on resonance with the laser, $\Delta_c \equiv \omega_l - \omega_c = 0$, so that, again, an atom decreases the cavity transmission. For a fixed flux of atoms, we count the number of dips dropping below an adjustable fraction $\mathcal{T}$ of the empty-cavity transmission. The dip number is normalized to the total number of fountain bursts. Experimental results for an atomic entrance velocity of 0.55 m/s and three different values of $\mathcal{T}$ are displayed in Fig. 2. It is obvious that lowering $\mathcal{T}$ reduces the number of dips below $\mathcal{T}$. Also, the number of dips decreases with increasing detuning, because farther away from the atomic resonance atomic absorption and dispersion are smaller. Assuming straight atomic trajectories, one would expect a decrease independent of the sign of the detuning Δ_a. However, this is not the case: the curves are asymmetric and the asymmetry between red and blue detuning is more pronounced for deeper dips.

To explain the existence of the asymmetry first, let us focus on the data for $\mathcal{T} = 5\%$. For red detuning ($\Delta_a < 0$), the dipole force pulls the atoms towards the antinodes so that the atoms channel through the high-coupling regions. This increases the probability of finding an atom close to an antinode and, hence, the number of deep dips. As the dipole force vanishes on the atomic resonance ($\Delta_a = 0$), the maximum number of dips is found for a small red detuning. For blue detuning ($\Delta_a > 0$) the atoms are pushed towards the weak-coupling regions close to the nodes, so that the number of dips decreases. This can be interpreted as a reflection in much the same way as atoms were predicted to be reflected from a cavity field in the one-dimensional model of Englert *et al.* [3]. The reason that the asymmetry disappears for larger $\mathcal{T}$ is that here most of the dips are due to atoms passing through the cavity farther away from the cavity axis. These atoms experience a weaker light force, with less impact on the atomic trajectory.

The curves in Fig. 2 show the results of a three-dimensional (3D) Monte Carlo (MC) simulation in which a large number ($\approx 10^4$) of trajectories is evaluated for point-like atoms. Their momentum obeys the differential equation $\dot{\vec{p}} = \vec{F}_d + \vec{F}_v + \dot{\vec{p}}_D$. The conservative dipole force [8] is $\vec{F}_d = -\hbar\eta^2\Delta_a\vec{\nabla}g(\vec{r})^2/\{[\Gamma\kappa + g(\vec{r})^2 - \Delta_a\Delta_c]^2 + [\Delta_a\kappa + \Delta_c\Gamma]^2\}$, with pump $\eta^2 = n_0(\kappa^2 + \Delta_c^2)$, and n_0 the empty-cavity photon number. The velocity-dependent force $\vec{F}_v = \vec{F}_v(\vec{r}, \vec{p})$ is a straightforward 3D extension of the lengthy 1D expressions for $\dot{z}f_1$ in Refs. [8], with

$\dot{z}(\nabla g)^2$ replaced by $(\dot{\vec{r}} \cdot \vec{\nabla} g(\vec{r}))\vec{\nabla} g(\vec{r})$. Note that $\vec{F}_v(\vec{r}, \vec{p})$ acts predominantly in the z direction. The diffusion has contributions from spontaneous emission (SE) and dipole fluctuations (DF), and is modeled by stochastic processes. The SE diffusion is 3D; the DF diffusion is important only in the cavity direction. In every time step Δt of the numerical integration of $\vec{p}$, a stochastic term $\Delta\vec{p}_D = \vec{S}(p_{max}^{SE}) + \hat{z}R(p_{max}^{DF})$ is added, where $\hat{z}$ is the unit vector along the cavity axis. $\vec{S}(\alpha)$ and $R(\beta)$ produce a uniformly distributed vector in a sphere of radius α and a random number between $-\beta$ and β, respectively, with $p_{max}^{SE} = [\frac{10}{3} D_{SE} \Delta t]^{1/2}$ and $p_{max}^{DF} = [6 D_{DF} \Delta t]^{1/2}$. In this way the diffusion satisfies the $[g(\vec{r})$, Δ_a, and $\Delta_c]$-dependent diffusion constants D_{SE} and D_{DF} given in Refs. [8]. Atoms are injected at $x = -3w_0$ randomly in the rectangle $(y, z) = (0 \ldots 2w_0, 0 \ldots \lambda/4)$. The initial velocity is upwards with a small (<1 cm/s) z component, to resemble the experimental situation. The effect of this component is noticeable only when diffusion is neglected in the simulation. The simulation returns atomic trajectories $\vec{r}(t)$ and the intracavity photon number $n(t)$. These results are confirmed by a second, independent, wave-function MC simulation, where the field and the atom's internal variables are treated fully quantum mechanically. In Fig. 2, the overall agreement between the simulation and the experimental results is very good. We also compared the data with a simulation based on the truncated equation $\dot{\vec{p}} = \vec{F}_d$, and the result (not shown) clearly disagreed with the data: it predicted a much larger asymmetry than actually seen in the experiment. This indicates that nonconservative forces are important to explain the data.

In order to obtain more information about the dynamics of the atomic motion, in particular the role of the different forces, we have measured the intensity autocorrelation function of the transmitted light, $g^{(2)}(\tau) = \langle I(t) I(t + \tau)\rangle / \langle I(t)\rangle^2$, where $I(t)$ is the intensity [14]. For each fountain burst we sample the bit stream from the photon-counting detector in $N = 20\,000$ bins $X(i)$ of 10 ns duration, giving a sample length of $T = 200$ μs. The technique covers the relevant time domain for the motional dynamics and is more convenient than start-stop measurements with two detectors. With the data of each of the 5×10^3 bursts an estimate of $g^{(2)}(\tau)$ is calculated:

$$\tilde{g}^{(2)}(\tau) \equiv \frac{1}{N - \epsilon} \sum_{i=1}^{N-\epsilon} \frac{X(i) X(i + \epsilon)}{\langle X\rangle^2}, \qquad \epsilon \equiv N\tau/T, \tag{1}$$

which takes into account the finite sample length. Here $0 < \tau \leq T$ is digitized in N time steps of size T/N, and the mean detector output $\langle X\rangle$ is averaged over 50 fountain bursts. The dead time of the detection circuit was measured to be 30 ns. This leads to a small deviation ($<2\%$ for our parameters) in $\tilde{g}^{(2)}(\tau)$. After correcting for this and averaging over all bursts, $g^{(2)}(\tau)$ is obtained.

Experimental results are shown in Fig. 3. The detunings $(\Delta_a, \Delta_c) = 2\pi \times (25, 5)$ MHz were chosen such that each atom passing through the cavity increases the cavity transmission: the transmitted intensity consists of bursts of photons with a duration determined by the vertical atomic velocity of 1.4 m/s. This leads to photon bunching, i.e., $g^{(2)}(\tau) > 1$, on a time scale of 20 μs, as is observed in the experiment. For longer times, the data tend to unity, indicating that photons are not correlated for $\tau > 50$ μs. The data also show a clear minimum at a correlation time of $\tau = 1$ μs, revealing a 0.5 MHz oscillation of the intracavity light intensity.

To get quantitative understanding of the data, $g^{(2)}(\tau)$ is calculated by substituting $n(t)$ from our simulation for X in Eq. (1). The simulation treats exactly one atom. In the experiment we have at most one atom strongly coupled to the cavity field. Because the features in $g^{(2)}(\tau)$ scale with the atomic flux, the vertical scale of the simulated curve is fitted to the data. As can be seen in Fig. 3, the result for $g^{(2)}(\tau)$ from the full simulation (solid line) matches the experimental data quite well. A simulation without any forces yields a curve which is flat below 5 μs (not shown). Setting $\dot{\vec{p}} = \vec{F}_d$, we get the dotted curve, which predicts but overestimates the minimum at 1 μs, and allows extra oscillations which are not seen in the data. Even worse, the simulated curve falls off much more slowly than the experimental data. These discrepancies disappear when $\dot{\vec{p}}_D$ is included in the simulation. The reason is that diffusion perturbs the oscillatory motion of the atom, thereby reducing the visibility of the oscillations in $g^{(2)}(\tau)$. The heating caused by the diffusion also makes the atom leave the cavity faster. This shifts the large bunching structure in the calculated $g^{(2)}(\tau)$ for $\tau < 50$ μs towards shorter times. Moreover, diffusion along the cavity axis produces atoms with enough axial velocity to run over the potential hills in the standing-wave field. These atoms induce a rapid field modulation, thereby

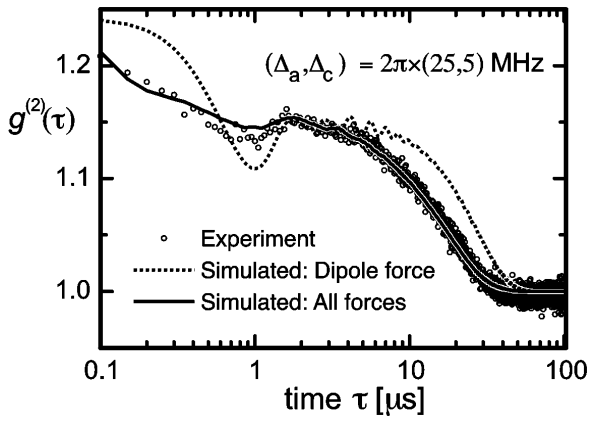

FIG. 3. Intensity autocorrelation function $g^{(2)}(\tau)$ of the transmitted light. Without atoms, the cavity contains 0.37 photons on average. The circles are data points. The dotted and solid lines are the results of a Monte Carlo simulation.

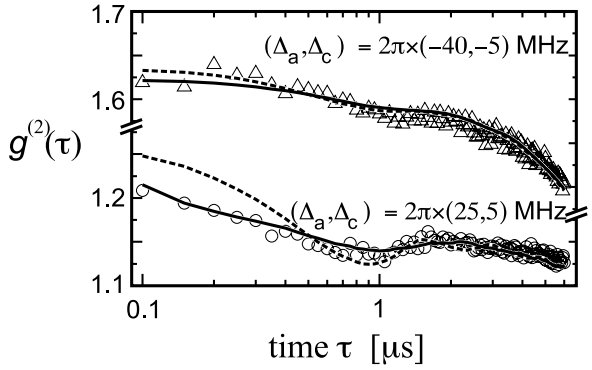

FIG. 4. Intensity autocorrelation function $g^{(2)}(\tau)$. The circles and triangles are data points. The corresponding solid (dashed) curves show the results of the simulation with (without) the velocity-dependent force, which heats and cools for the parameters of the lower and upper curves, respectively.

changing the bunching feature in $g^{(2)}(\tau)$ at short time intervals. However, diffusion alone cannot explain the feature observed for $\tau < 0.5\ \mu$s quantitatively, so that $\vec{F}_v$ must be taken into account to get the good match between the data and the simulation, as is explained now.

To exemplify the effect of the velocity-dependent force $\vec{F}_v$, the measurement for $(\Delta_a, \Delta_c) = 2\pi \times (25, 5)$ MHz (from Fig. 3) is now compared with a measurement for $(\Delta_a, \Delta_c) = 2\pi \times (-40, -5)$ MHz. Results are depicted in Fig. 4. The overall difference in amplitudes between the two measurements stems from the force on the atoms towards or away from the antinode, leading to higher or lower average cavity transmission, respectively, in combination with a slightly different atom flux. More important is that, for $\tau < 0.5\ \mu$s, $g^{(2)}(\tau)$ decays much faster for the blue-detuning data (circles) than for the red-detuning data (triangles). Quantitatively, this difference cannot be attributed to a change of the diffusion caused by, e.g., a different Δ_a. There is, however, a significant difference in $\vec{F}_v$: a straightforward analysis based on the Sisyphus picture discussed in the introduction suggests that this force heats/cools for our blue/red−detuning parameters. Indeed, when including this force in the simulation, good agreement with experimental data is obtained. For the blue-detuning parameters, the difference between the dashed curve (without $\vec{F}_v$) and the solid curve (with $\vec{F}_v$) indicates how $\vec{F}_v$ heats the atoms in the axial direction. For the red-detuning parameters this heating is absent, so that leaving out $\vec{F}_v$ hardly changes the simulated curve. In fact, here $\vec{F}_v$ is predicted to cool almost optimally, but as the axial velocity of the atoms is already very small, the effect of cooling is negligible. For this reason, it will be very difficult to observe cooling in the present setup. However, we emphasize that the heating effect deduced from the short-term behavior of $g^{(2)}(\tau)$ for the blue-detuning parameters is caused by the same cavity-mediated Sisyphus mechanism.

In conclusion, we have clear evidence for channeling and diffusive heating of atoms in the standing wave of a high-finesse optical cavity containing less than one photon on average. Moreover, the better agreement between the measured and calculated intensity autocorrelation function, which is found when all forces predicted in Refs. [8] are included in the simulation, gives first evidence for the existence of the new cavity-mediated velocity-dependent force. Once this force is fully mastered, it can be employed to cool and trap an atom in a high-finesse cavity. Besides fundamental interest in the exploration of the Jaynes-Cummings system, a single cold atom stored in an antinode of the cavity mode is an ideal system to create entangled atom-photon states for applications in, e.g., quantum information processing.

We thank H. Ritsch and M. Gangl for valuable discussions. This research was supported by the Deutsche Forschungsgemeinschaft, the Optikzentrum Konstanz, and the TMR network "Microlasers and Cavity QED." P. W. H. P. acknowledges a TMR grant from the EU.

[1] See, e.g., *Cavity Quantum Electrodynamics*, edited by P. R. Berman (Academic Press, San Diego, 1994).
[2] B. W. Shore, P. Meystre, and S. Stenholm, J. Opt. Soc. Am. B **8**, 903 (1991).
[3] B.-G. Englert, J. Schwinger, A. O. Barut, and M. O. Scully, Europhys. Lett. **14**, 25 (1991).
[4] S. Haroche, M. Brune, and J. M. Raimond, Europhys. Lett. **14**, 19 (1991).
[5] M. O. Scully, G. M. Meyer, and H. Walther, Phys. Rev. Lett. **76**, 4144 (1996).
[6] C. J. Hood, M. S. Chapman, T. W. Lynn, and H. J. Kimble, Phys. Rev. Lett. **80**, 4157 (1998); H. Mabuchi, J. Ye, and H. J. Kimble (to be published).
[7] A. C. Doherty, A. S. Parkins, S. M. Tan, and D. F. Walls, Phys. Rev. A **56**, 833 (1997).
[8] P. Horak, G. Hechenblaikner, K. M. Gheri, H. Stecher, and H. Ritsch, Phys. Rev. Lett. **79**, 4974 (1997); G. Hechenblaikner, M. Gangl, P. Horak, and H. Ritsch, Phys. Rev. A **58**, 3030 (1998).
[9] J. Dalibard and C. Cohen-Tannoudji, J. Opt. Soc. Am. B **2**, 1707 (1985).
[10] Improved laser cooling, employing the spontaneous-emission enhancement in a cavity, is predicted in T. W. Mossberg, M. Lewenstein, and D. J. Gauthier, Phys. Rev. Lett. **67**, 1723 (1991).
[11] P. Münstermann, T. Fischer, P. W. H. Pinkse, and G. Rempe, Opt. Commun. **159**, 63 (1999).
[12] G. Rempe, Appl. Phys. B **60**, 233 (1995); R. Quadt, M. Collett, and D. F. Walls, Phys. Rev. Lett. **74**, 351 (1995).
[13] H. Mabuchi, Q. A. Turchette, M. S. Chapman, and H. J. Kimble, Opt. Lett. **21**, 1393 (1996).
[14] Single atoms in a MOT have been studied with a photon correlation technique by V. Gomer, F. Strauch, B. Ueberholz, S. Knappe, and D. Meschede, Phys. Rev. A **58**, R1657 (1998).